Diakoptic Analysis of Electromagnetic Systems

Dragan I. Olćan, *Member, IEEE*, Antonije R. Djordjević

***Abstract* — This paper presents an efficient general method for the numerical analysis of complex and large electromagnetic-field structures. The method is based on merging the diakoptic approach with the surface integral equation formulations. Compared to the classical integral equation approach, the proposed method provides significant reduction of the CPU time and storage, preserving high accuracy of results.**

***Keywords* — Electromagnetic analysis, Diakoptics.**

I. Introduction

FOR several decades, numerical techniques have been successfully used to solve electromagnetic (EM) field problems. We focus our attention on EM systems that are made of linear isotropic and piecewise-homogeneous materials, which is a reasonable assumption for most practical applications. Particularly efficient and accurate are integral equation formulations. They are based on the boundary conditions, and they are usually solved using the method of moments (MoM) [1]-[6]. For the class of problems considered, the unknowns in these equations are surface sources. Hence, we talk here about surface integral equation (SIE) formulations. From our experience, the SIE approach is substantially more efficient and accurate than using the finite-difference method (FD) and the finite-element method (FEM) [4]-[6]. The advantage of the SIE approach is most significant for open-region problems (e.g., antennas, multiconductor transmission lines without shields, etc.).

There is an ever-increasing demand to analyze larger and more complex structures, leading to tremendous increase of storage and CPU time requirements. This, in turn, calls for development of new numerical techniques that can meet these demands on available computers. Various approaches based on domain decomposition and equivalent sources have been used to increase the efficiency of computations of the FD, FEM, and MoM techniques. Notable examples are the domain decomposition method [7]-[9], the fast multipole method [10], [11], and several approaches with multilevel basis functions [12], [13]. Huge accelerations of the finite-difference and finite-element formulations using the partitioning have been reported in [14], [15]. In [16], [17], an approach has been developed to improve the efficiency of the integral equation analysis of scatterers based on Huygens' principle, volume integral equations, and partitioning.

The ideas presented in these papers have motivated us to merge the advantages of the SIE formulations and the domain partitioning (diakoptic approach), with the goal to develop an efficient general method for the analysis of complex and large EM systems. We will refer to this method as the diakoptic approach with surface integral equations (DSIE). We have successfully applied this method to the analysis of two-dimensional (2-D) and three-dimensional (3-D) EM systems, both in electrostatic and dynamic fields [18]-[22].

The remainder of the paper is organized as follows. Section II summarizes an equivalence theorem that is the foundation for the diakoptic approach and MoM-SIE. The DSIE approach itself is outlined in Section III. Details of its combination with the SIE formulations are given in Section IV. Section V presents some examples of the DSIE analysis of electrostatic and dynamic problems. Finally, Section VI provides concluding remarks.

II. Equivalence Theorem

In the theory of electromagnetic fields, there exist several equivalence theorems [23], [24]. The DSIE approach is based on the theorem of equivalent surface sources (Huygens' principle). We summarize the statement of this theorem, without the strict proof.

Let us consider the general case of the dynamic EM field (Fig. 1a). One part of the region where the EM field exists is wrapped by an arbitrary closed surface S. The inward normal on that surface is $\mathbf{n}$, while $\mathbf{E}_1$ and $\mathbf{H}_1$ are the electric and magnetic fields inside S. Let us place fictitious surface electric currents (of density $\mathbf{J}_s$) and surface magnetic currents (of density $\mathbf{M}_s$) on S. The equivalence theorem claims that if $\mathbf{J}_s = \mathbf{n} \times \mathbf{H}_1$ and $\mathbf{M}_s = -\mathbf{n} \times \mathbf{E}_1$, and if all field excitations outside S are turned off, then the EM field inside S is preserved, while the EM field outside S is annihilated (Fig. 1b). The surface currents $\mathbf{J}_s$ and $\mathbf{M}_s$ are referred to as equivalent sources.

If the sign of the equivalent sources is changed (or, equivalently, if the direction of the unit normal $\mathbf{n}$ is reversed) and if all excitations inside S are turned off, the field outside S is preserved, while the field inside S is annihilated (Fig. 1c).

This work has been supported in part by the COST Action IC0603 (Assist) and by the Grant TR 11021 of the Serbian Ministry of Science and Technological Development.

D. I. Olćan, School of Electrical Engineering, University of Belgrade, Serbia (phone: 381-(0)11-3218.353; e-mail: olcan@etf.rs).

A. R. Djordjević, School of Electrical Engineering, University of Belgrade, Serbia (phone: 381-(0)11-3218.329; e-mail: edjordja@etf.rs)

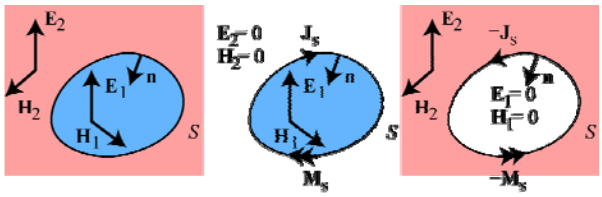

(a) (b) (c)

Figure 1. Equivalence theorem: (a) original system and equivalent systems for (b) interior and (c) exterior regions.

There are surface electric and magnetic charges associated with the equivalent currents. The charge densities can be evaluated using the continuity equations: $\mathrm{div}_s \mathbf{J}_s = -j\omega\rho_s$ for the electric charges and $\mathrm{div}_s \mathbf{M}_s = -j\omega\tau_s$ for the magnetic charges.

In the electrostatic case, the equivalent surface sources reduce to surface charges (of density ρ_s) and surface dipoles (i.e., a double-charge layer, of density $\mathbf{p}_s$) [23]. Referring to Fig. 1b, these equivalent sources are evaluated as $\rho_s = \varepsilon_0 E_n = -\varepsilon_0 \frac{\partial V}{\partial n}$ and $\mathbf{p}_s = \varepsilon_0 \mathbf{n} V$, where V_1 is the electric scalar-potential inside S. The density of the surface dipoles is a vector perpendicular to S. It can be represented as $\mathbf{p}_s = p_s \mathbf{n}$, where p_s is the projection of $\mathbf{p}_s$ on $\mathbf{n}$.

III. Diakoptic Approach

The diakoptic approach (domain partitioning) has been successfully used over years in various areas, like the circuit theory [24], networking [25], and to some extent in EM analysis [12], [26]-[29].

In our diakoptic approach, the analyzed EM system is split into non-overlapping arbitrarily-shaped subsystems. The union of all subsystems is the whole region of interest (i.e., the space with non-zero EM field in the original problem). The boundary of a subsystem is a virtual closed surface (diakoptic surface), which is an interface between the subsystem and its environment.

Equivalent surface sources are placed on the diakoptic surface. Each subsystem, along with the corresponding equivalent surface sources, is analyzed independently of other subsystems. The analysis can be carried out using the FD, FEM, or SIE/MoM approaches. The objective of the analysis is to find a relation between the equivalent sources at the diakoptic surface. This relation is linear, and it includes contributions of the excitations located in the subsystem. It can be written in matrix form. This relation is valid for any EM environment in which the subsystem may be located.

There are various possibilities to set this matrix relation. The formulation shown here is analogous to the Norton representation of a multiport linear network. However, other formulations are possible, e.g., analogous to the Thevenin representation or the scattering-parameter representation of a multiport network. The latter formulation is advantageous in dynamic cases as it helps suppress parasitic resonances of the analyzed subsystem.

The relations for all subsystems are combined into a system of linear equations (diakoptic system of equations) to yield the equivalent sources at the diakoptic surfaces. Once these sources are found, the EM field in the original problem can be calculated for each subsystem using the equivalent sources at its diakoptic surface and the excitations within the subsystem.

Each subsystem is substantially smaller and simpler than the original system. Hence, the diakoptic solution can be more efficient than the simultaneous solution of the original EM system.

IV. Diakoptic Approach Combined With Surface Integral Equation Formulations

A. Diakoptic Implementation

Our objective is to analyze an arbitrary (linear) EM system made of piecewise-homogeneous linear isotropic materials. Following the classical MoM approach, the problem is most efficiently solved using surface integral equation formulations [4], based on the surface equivalence theorems. The unknowns are surface equivalent sources at the surfaces of material discontinuities (e.g., conductor surfaces and dielectric-to-dielectric interfaces). In a dynamic case, the equivalent sources are surface electric and magnetic currents. In an electrostatic case, the equivalent sources are surface electric charges (along with surface dipoles in some formulations).

Instead of applying MoM to the whole analyzed system, we employ the diakoptic approach. For each subsystem, we postulate boundary conditions for all surfaces of material discontinuities, as well as for the diakoptic surface. Based on these conditions, we formulate a set of surface integral equations. The unknowns are the equivalent sources at the material boundaries (the same sources as in the classical approach) and the equivalent sources at the diakoptic boundaries.

MoM is thereafter applied to each subsystem. All equations and unknowns are treated in a unique way. In particular, we use the same expansion functions for all equivalent sources, to simplify the programming implementation. However, there is no theoretical obstacle to use different expansion functions.

The proposed technique is general and applicable to various two-dimensional and three-dimensional problems. The region of a subsystem can be finite or infinite. Hence, the approach can be applied both to open-region and boxed problems.

For simplicity, we further describe the diakoptic formulation in more details only for the electrostatic case, because the equivalent sources are expressed in terms of scalar quantities.

We consider a large electrostatic system that consists of arbitrarily shaped conductors and piecewise-homogeneous dielectrics. The dimensions of the system, the material properties, and the potentials of all conductors are assumed known. The objective is to evaluate the charge

distribution on the conductors due to the given excitations (potentials).

In the classical MoM approach, the problem can be solved using a surface integral equation formulation [5], [30]. Applying the concept of bound charges, the medium is homogenized and reduced to a vacuum. A set of surface integral equations is formulated for the total surface charges on the surfaces of the material discontinuities. These equations are based 1) on the boundary condition for the potentials at the conductor surfaces, and 2) on the condition for the normal component of the electric field at the dielectric-to-dielectric interfaces. MoM is thereafter applied to find the distribution of the total charges. Finally, the free surface charges on the conductors are extracted from the total charges.

In the diakoptic formulation, the unknowns are the total surface charges on the surfaces of material discontinuities along with the equivalent surface charges and dipoles on the diakoptic surfaces. We formulate the same surface integral equations for the surfaces of the material discontinuities as in the classical approach. For each diakoptic surface, we formulate an additional surface integral equation by requiring that the potential is zero just outside the corresponding subsystem. This equation has the same form as classical surface integral equations for a conductor. Compared to the classical formulation, we have one additional straightforward task: to evaluate the potential and electric field due to the surface dipoles.

For simplicity, let us consider that the original problem is split into only two subsystems (Fig. 2a). An arbitrarily shaped closed surface S represents the boundary between these two subsystems. The first subsystem consists of the structure inside S (Fig. 2b), and the second subsystem consists of structure outside S (Fig. 2c). We apply MoM to each subsystem. In particular, we use a piecewise-constant approximation of the unknowns, i.e., the basis functions are constants (pulses) defined on respective subsections (patches).

The total number of patches for the approximation of the charge distribution on the surfaces of material discontinuities in a subsystem is N_i, $i = 1,2$. There is one unknown charge coefficient per patch. The total number of patches for the diakoptic surface is D. For each patch on this boundary, there are two unknown coefficients (scalars): one for the surface charges (ρ_s) and one for the intensities of surface dipoles (p_s). Hence, the total number of unknowns for the diakoptic boundary is $2D$.

Note that it is not necessary to apply the same patching scheme for the surface charges and the surface dipoles on the subsystem boundary. It is sufficient that the same number of unknown coefficients is used for the surface charges and the surface dipoles. Consequently, the DSIE method can be implemented with higher-order basis functions as well.

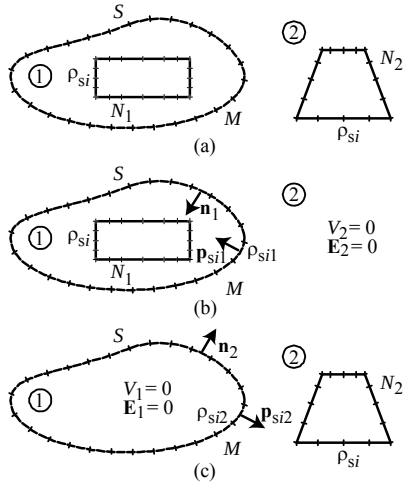

Figure 2. Domain partitioning for the case of two subsystems: (a) original system, (b) subsystem 1, and (c) subsystem 2.

For each subsystem, we evaluate a linear relation between the unknown coefficients for ρ_s and p_s at the diakoptic surface. These relations have the common form

$$[\boldsymbol{\rho}_{si}] = [\mathbf{y}_i][\mathbf{p}_{si}] + [\boldsymbol{\rho}_{si}]_0, \; i = 1,2, \tag{1}$$

where $[\boldsymbol{\rho}_{si}]$ and $[\mathbf{p}_{si}]$ are column-matrices that contain the coefficients for the pulse approximations of ρ_s and p_s at the subsystem (diakoptic) boundary, respectively, $[\boldsymbol{\rho}_{si}]_0$ is a column-matrix that is due to the excitations in the subsystem, and $[\mathbf{y}_i]$ is a square matrix. The dimensions of matrices $[\boldsymbol{\rho}_{si}]$, $[\mathbf{p}_{si}]$, and $[\boldsymbol{\rho}_{si}]_0$ are $D \times 1$, while the dimensions of $[\mathbf{y}_i]$ are $D \times D$.

For each subsystem, matrix $[\boldsymbol{\rho}_{si}]_0$ is evaluated by setting to zero the intensities of all surface dipoles. The conductors in the subsystem are on their original potentials, and the potential at the diakoptic surface is zero.

Matrix $[\mathbf{y}_i]$ is calculated when the potentials of all conductors are set to zero, and the system is exited by one surface dipole (pulse) at a time. We assume that the intensity of the surface dipole on one patch is unit, and we compute the coefficients for the surface charges at the diakoptic surface and at all surfaces of material discontinuities in the subsystem. Numerically, the coefficients of the charges at the diakoptic surface give one column of $[\mathbf{y}_i]$. As a byproduct of this analysis, the coefficients of the pulse approximation for the surface charges on the conductors, $[\boldsymbol{\rho}_{sci}]$, are related to $[\mathbf{p}_{si}]$ as $[\boldsymbol{\rho}_{sci}] = [\mathbf{c}_i][\mathbf{p}_{si}] + [\boldsymbol{\rho}_{sci}]_0$, where $[\mathbf{c}_i]$ is an $N_c \times D$ matrix and N_c is the total number of coefficients for the free charges on the conductors.

For the computation of matrices $[\boldsymbol{\rho}_{si}]_0$, $[\mathbf{y}_i]$, and $[\mathbf{c}_i]$, the MoM system matrix for a subsystem is filled and LU decomposed only once. The results are obtained using LU

back-substitutions for various excitations.

The equivalent sources at the diakoptic surface are opposite for the two subsystems. Taking into account the opposite directions of the perpendicular unit vectors $\mathbf{n}_1$ and $\mathbf{n}_2$, we can write

$$[\boldsymbol{\rho}_{s1}] = -[\boldsymbol{\rho}_{s2}] \quad \text{and} \quad [\mathbf{p}_{s1}] = [\mathbf{p}_{s2}] = [\mathbf{p}_s]. \tag{2}$$

Combination of (1) and (2) yields the diakoptic system of D linear equations,

$$([\mathbf{y}_1] + [\mathbf{y}_2])[\mathbf{p}_s] = -[\boldsymbol{\rho}_{s1}]_0 - [\boldsymbol{\rho}_{s2}]_0 . \tag{3}$$

Once $[\mathbf{p}_s]$ is calculated from (3), matrices $[\boldsymbol{\rho}_{si}]$, $i = 1,2$, are calculated from (1). The conductor charges in the subsystems are calculated using matrices $[\mathbf{c}_i]$.

When evaluating the matrix of electrostatic-induction coefficients for a multiconductor electrostatic system, the charge distribution has to be calculated several times, for various excitations (i.e., for different conductor potentials). In that case, the diakoptic system matrix is formed only once and then it is LU decomposed. The conductor potentials affect only the right-hand side in (3). The corresponding matrices $[\boldsymbol{\rho}_{si}]_0$ are calculated and the LU back-substitution is performed to find $[\mathbf{p}_s]$ as many times as needed.

For the dynamic case, the diakoptic formulation is similar. The major difference is that now we have surface electric currents at the diakoptic surfaces (instead of the surface charges) and surface magnetic currents (instead of the surface dipoles). These currents are vector quantities. Each of them can be represented in terms of two components (tangential to the surface), which are scalar quantities. Following the same principles as for the electrostatic case, we formulate a matrix relation between the components of the equivalent surface currents and the equivalent surface magnetic currents. We can use arbitrary patching schemes for these currents, and the only constraint is that we have the same total number of unknowns for both equivalent current distributions.

B. Maximal Theoretical Efficiency of the Diakoptic Approach

We now estimate the efficiency of the diakoptic formulation assuming single-level decomposition. First, we consider a boxed EM system that is split into K congruent subsystems. Referring to the electrostatic case, let us denote by N the total number of unknowns for surfaces of material discontinuities in a subsystem. Let D be the total number of unknown coefficients for ρ_s on the diakoptic boundary of the subsystem. The number of unknown coefficients for p_s is also D. Hence, when compared to the classical solution, the number of additional unknowns for a subsystem is $2D$. The coefficients for ρ_s and p_s on the diakoptic surface are related as in (1).

The total number of unknowns for solving the whole structure using the classical MoM procedure is KN. In the diakoptic approach, the total number of unknowns for the MoM analysis of one subsystem is $N + D$. If the subsystems are congruent, it is sufficient to analyze only one subsystem since the matrix relation (1) is identical for all of them. The total number of unknowns in the diakoptic system of linear equations is KD.

We suppose that the CPU time required for the matrix inversion dominates in the numerical solution. The time needed for solving a system of linear equations is proportional to the cube of the total number of unknowns. We estimate the acceleration of the diakoptic analysis as

$$a = \frac{t_{\mathrm{SIE}}}{t_{\mathrm{DSIE}}} \approx \frac{(KN)^3}{(N+D)^3 + \alpha(KD)^3}, \tag{4}$$

where t_{SIE} is the CPU time needed for the classical MoM-SIE approach, t_{DSIE} is the time for the DSIE approach, and $\alpha = 1$. Fig. 3 shows the acceleration as a function of N/D, with K as a parameter. By inspecting Fig. 3, we see that for fixed K, there is no use of increasing N/D above a certain value ($N/D \approx K$). For fixed N/D, the maximal acceleration (when K increases) is $a_{\max} = \lim_{K\to\infty} a = (N/D)^3/\alpha$. We also note that the diakoptic formulation can be useful even with $K = 2$.

The computer memory required to store a system of linear equations is proportional to the total number of unknowns squared. Assuming this memory requirement to dominate, we estimate the memory efficiency as

$$m = \frac{m_{\mathrm{SIE}}}{m_{\mathrm{DSIE}}} \approx \frac{(KN)^2}{(N+D)^2 + \alpha(KD)^2}, \tag{5}$$

where m_{SIE} is the storage needed for the classical MoM, m_{DSIE} is the storage for the diakoptic analysis, and $\alpha = 1$. The maximal memory efficiency of the diakoptic formulation when $K \to \infty$ is $m_{\max} = (N/D)^2/\alpha$.

Let us consider now an open-region system and let K be the total number of congruent subsystems. The total number of subsystems is $K+1$ because we have an infinite-region subsystem (note that its diakoptic surface is finite), which is different from other subsystems. In the worst case, the total number of unknown coefficients for the diakoptic surface of this subsystem is KD. The acceleration and the memory efficiency of the diakoptic formulation are given by (4) and (5), respectively, with $\alpha = 2$.

Generally, if $D << N$, the diakoptic formulation will solve the problem faster and with less memory resources than the classical MoM approach. The diakoptic boundaries should be located in regions where the EM field is a slowly-varying function of spatial coordinates. All regions with fast-varying fields, which include fine

details of the analyzed structure, should be kept within subsystems and away from the diakoptic surfaces. This strategy enables the ratio N/D to be large enough without sacrificing the accuracy of results. Consequently, the more complex the EM system is, the more efficient is the diakoptic formulation.

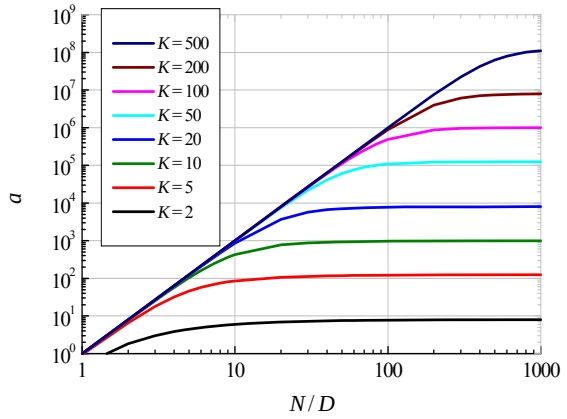

Figure 3. Acceleration obtained by DSIE.

The diakoptic formulation is most efficient when all subsystems are congruent. Nevertheless, it can also be used efficiently when subsystems are non-congruent. Partitioning into subsystems can also be performed using multilevel (nested) schemes. The diakoptic formulation can be implemented on parallel processors, so that subsystems are analyzed simultaneously. Nesting and parallelization further increase the efficiency of the DSIE formulation.

V. Numerical Examples

The aim of examples presented in this section is to demonstrate the efficiency that can be achieved using DSIE, i.e., the acceleration and the storage reduction when compared to the classical MoM-SIE solution. The accuracy of the diakoptic approach is also considered.

A. 2-D Electrostatics

The first example demonstrates the diakoptic approach in conjunction with the 2-D electrostatic analysis. The structure is a motherboard bus with 16 microstrip lines located in a vacuum. The cross-section is shown in Fig. 4. The widths and heights of all strips are identical, $w = 3\,\text{mm}$ and $h = 0.5\,\text{mm}$, respectively. All strips are infinitely thin. The separation among neighboring strips is $s = 3\,\text{mm}$. There are 256 unknowns per each strip, i.e., 4096 unknowns for the whole structure. The cross-section of the subsystem boundaries for the diakoptic approach is colored gray in Fig. 4. There are 17 subsystems in total: 16 of them consist of a single strip along with encompassing walls, while the last one is the outer space. The height of the encompassing wall is $H = 1.5\,\text{mm}$ while its width is 4 times larger. The total number of pulses for the wall contour is D. Since this is the open-region problem, the last subsystem is computationally the most complex one.

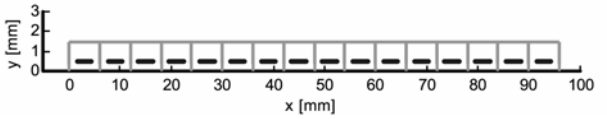

Figure 4. Cross-section of the bus with 16 microstrips in a vacuum.

The maximal relative error in the matrix of electrostatic induction coefficients [**B**], and the acceleration are in focus. Results are summarized in Table 1. The first column of the table is the number of diakoptic unknowns around one strip, the second column is the maximal relative error, and the last column shows the acceleration.

The results in Table 1 show that the diakoptic approach provides very large CPU time improvement. For the maximal relative error on the order of 10^{-2} (1%) the CPU time improvement is about 2000 times.

Table 1: Acceleration and Error of Diakoptic Approach.

D	Maximal relative error	Acceleration
5	2.8e–2	**2532**
10	8.3e–3	**1758**
20	2.6e–3	**711**
40	8.1e–4	**108**
80	2.6e–4	**14**
120	8.4e–5	**1.8**

B. 3-D Electrostatics

The second example demonstrates the diakoptic approach in conjunction with 3-D electrostatic analysis. The geometry of the analyzed system is shown in Fig. 5a. It consists of two square metallic plates (the side is $40\,\text{mm}$), located on the surface of a dielectric slab ($160\,\text{mm} \times 240\,\text{mm} \times 2\,\text{mm}$). The relative permittivity of the dielectric is $\varepsilon_r = 5$. In the classical approach, the system is analyzed by formulating a set of integral equations for the total charges (free plus bound charges) as in [5], [30], and solving the equations using MoM with a piecewise-constant approximation for the charge distribution on a set of triangles. Thereby, each metallic plate is divided into 400 triangles, and the dielectric-to-vacuum interfaces are divided into 2800 triangles.

In the diakoptic analysis, the system is divided into three subsystems, as shown in Fig. 4b-d. The two interior subsystems are congruent. Each subsystem contains one metallic plate and a part of the dielectric slab. The diakoptic boundary is a rectangular box (which is patched into D triangles). The diakoptic surfaces for these two subsystems share a common wall. The exterior subsystem contains a part of the dielectric slab because the diakoptic surfaces intersect the slab at a distance of $20\,\text{mm}$ from the edges of the metallic plates.

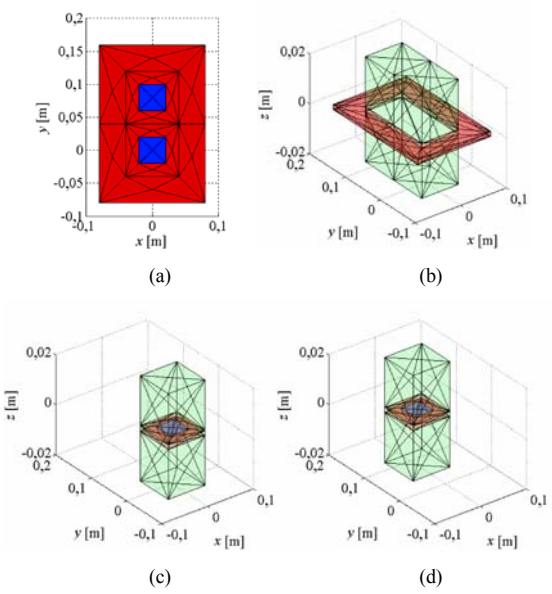

Figure 5. Two metallic plates on dielectric slab: (a) original system, (b) exterior diakoptic subsystem, and (c), (d) interior diakoptic subsystems.

For the number of triangles on a diakoptic surface 400, the relative error is 1%, the acceleration is $a \approx 3$ times, and the memory reduction is slightly greater than 1. This example demonstrates that the diakoptic boundaries of the subsystems can cut the original EM structure without compromising the final results.

C. 2-D Electrodynamics

The third example demonstrates the diakoptic approach in conjunction with 2-D TM electrodynamic analysis. For the purpose of comparison, the matrix parameters for a multiconductor line are calculated by the classical analysis and by the DSIE formulation. A flat cable with 26 identical conductors is used as a real-life example of multiconductor transmission lines. The cross-section of the cable is shown in Fig. 6. The radius of a conductor is $r_c = 0.254\,\text{mm}$. The radius of a dielectric coating is $r_d = 0.4\,\text{mm}$. Conductor axes reside in one plane with the spacing $p = 1\,\text{mm}$. The PVC dielectric coating is lossy, its relative permittivity is $\varepsilon_r = 3.3$, and the loss tangent is $\tan\delta = 0.005$. The conductance of conductors is $\sigma = 56\,\text{MS/m}$ (copper). The permeability is $\mu = \mu_0$ everywhere. The matrix parameters for the cable are calculated at $f = 1\,\text{MHz}$, where the skin-effect is already pronounced.

In the classical electrostatic analysis, we take equal numbers of uniform pulses per the circumference of each conductor and dielectric coating. The total number of unknown coefficients (for the total charges) for one conductor and its coating is a) $N = 64$ and b) $N = 192$. In the classical TM dynamic analysis, the total number of unknown coefficients for the electric and magnetic currents for one conductor is a) $N = 64$ and b) $N = 192$ (the same as in the electrostatic case).

In the DSIE analysis, the system is partitioned into 27 subsystems: 26 consist of one conductor with the dielectric coating, while the last subsystem is the remaining infinite region. The diakoptic boundary surfaces are placed coaxially with the conductors. The cross-section of a diakoptic surface is taken to be a square whose side is $w = 0.9\,\text{mm}$ (Fig. 6). Consequently, we have 26 congruent subsystems, each consisting of a conductor, its coating, and a diakoptic boundary. The last subsystem consists of the outer region and the union of all diakoptic boundaries. The patching scheme for the subsystems is the same as for the classical MoM analysis. The total number of uniform pulses per circumference of a diakoptic surface, M, is varied. In both the classical SIE and the DSIE analysis, the last (26^{th}) conductor is the reference.

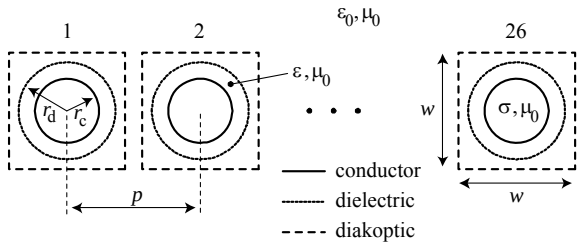

Figure 6. Cross section of a flat cable.

The accuracy of the DSIE formulation, compared to the classical SIE analysis, is estimated using the maximal relative error for matrices $[\mathbf{B}']$ and $[\mathbf{Z}'] = [\mathbf{R}'] + j\omega[\mathbf{L}']$. The maximal relative error for matrix $[\mathbf{B}']$ is calculated as $\delta[\mathbf{B}'] = \max\left(\left| b_{ij}^{\text{SIE}} - b_{ij}^{\text{DSIE}} \right| \Big/ \left| b_{ij}^{\text{SIE}} \right|, i, j = 1,2,...,25 \right)$, where b_{ij}^{SIE} is the element in the i-th row and j-th column of matrix $[\mathbf{B}']$ calculated by the MoM-SIE analysis and b_{ij}^{DSIE} is the corresponding element calculated by the DSIE analysis. (Errors in matrices $[\mathbf{B}']$ and $[\mathbf{G}']$ practically coincide.) The maximal relative error for matrix $[\mathbf{Z}']$ is calculated in the same manner.

The CPU time and the occupied memory were measured for the classical SIE analysis and the DSIE formulation. The acceleration of the DSIE formulation is calculated as $a = t_{\text{SIE}} / t_{\text{DSIE}}$ and the memory efficiency is calculated as $m = s_{\text{SIE}} / s_{\text{DSIE}}$.

Results are shown in Fig. 7. The maximal relative error (Fig. 7a), the acceleration (Fig. 7b), and the memory efficiency (Fig. 7c) are plotted versus M. A small value of M is sufficient to provide a very good accuracy. Increasing M decreases the maximal relative errors in matrices $[\mathbf{B}']$ and $[\mathbf{Z}']$, but also decreases the acceleration and the memory efficiency. The results verify that the DSIE formulation is more efficient for subsystems that are more complex.

Comparison of results shown in Figs. 7b and 7c with the corresponding estimations (4) and (5), for $\alpha = 2$, shows that the estimations agree fairly well (within 50%

for $M \le 32$) with the measured results.

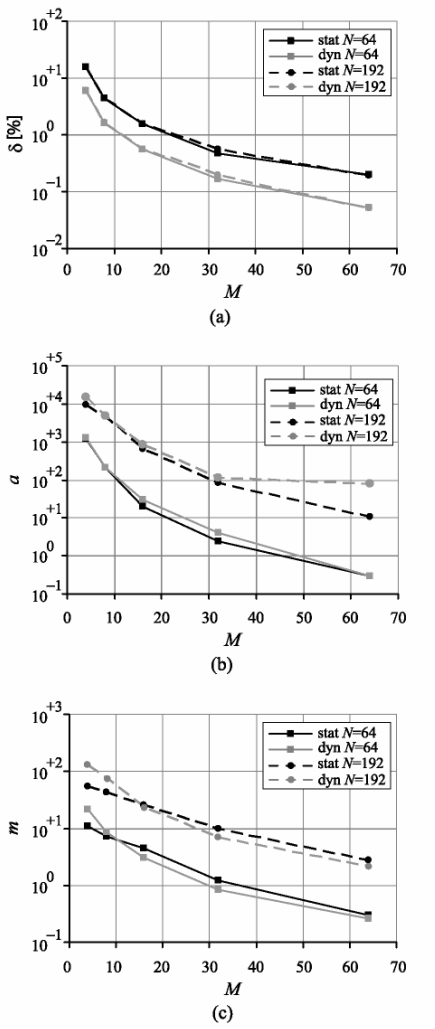

Figure 7. Comparison between DSIE and classical SIE for electrostatic (stat) and TM dynamic (dyn) analyses: (a) maximal relative error, (b) acceleration, and (c) memory efficiency.

D. 3-D Electrodynamics

The last example demonstrates the diakoptic approach in conjunction with 3-D electrodynamic analysis. It is a scatterer that consists of 1250 identical metallic cubes grouped in 10 clusters (Fig. 8a). A cluster consists of 125 ($5\times5\times5$) metallic cubes (Fig. 8b). The side of a cube is $a = 1\,\text{mm}$. The distance between neighboring cubes in a cluster is $d = 1\,\text{mm}$ in the x , y , and z -directions. The distance between neighboring clusters is $p = 6\,\text{mm}$ in the y - and z -directions. The illuminating EM wave arrives from the direction $\phi = 0$, $\theta = 0$. The rms value of the incident electric field is $E = 1\,\text{V/m}$ and the electric field vector is parallel to the z-axis. The frequency of the incident EM wave is $f = 15\,\text{GHz}$. The electrical length of the cube side is $\lambda/20$, where λ is the free-space wavelength. The dimensions of one cluster are $9\lambda/20\times9\lambda/20$, and the dimensions of the whole scatterer are $9\lambda/20\times3.5\lambda\times1.25\lambda$. The number of the unknown coefficients (for the electric current expansions) for one metallic cube is 12, which amounts to $N_{\text{tot}} = 15\,000$ for the whole scatterer.

For the DSIE approach, the scatterer is divided into 11 subsystems. The first one consists of the outer space and the diakoptic boundaries of the other 10 subsystems (Fig. 7a). The remaining 10 subsystems are congruent. Each of them consists of a cluster of 125 cubes wrapped by a diakoptic boundary (Fig. 7b). The diakoptic boundary is a cube of a side $b = 11\,\text{mm}$. The total number of the unknown coefficients for the current expansions of the equivalent electric (magnetic) currents on the diakoptic boundary is $D = 192$ and for the encapsulated cluster is $N = 1500$. Since we have 10 congruent subsystems, their diakoptic matrices are identical. Therefore, we solve only two subsystems with MoM/SIE: the exterior one and one of the interior subsystems.

The RCS calculated with the classical MoM/SIE and the DSIE formulations is shown in Fig. 9 for the cut $\theta = 2^\circ$. The results calculated using DSIE and MoM/SIE match very well.

The simulation of the whole scatterer at once using WIPL-D [6] out-of-core solver lasts $t_{\text{SIE}} = 7615\,\text{s}$ on a 32-bit desktop PC with 1 GB of RAM. On the same PC, the DSIE simulation takes $t_{\text{DSIE}} = 624\,\text{s}$. Therefore, the achieved acceleration is $a = 12.2$ times. This result is somewhat conservative since the non-optimized diakoptic code is compared to a professional and highly optimized commercial code [6]. The estimated acceleration from eqn. (4) is $a = 177.6$.

To store the MoM/SIE matrix of the whole scatterer (double precision complex numbers) takes $m_{\text{SIE}} = 3.6\,\text{GB}$. That amount of memory was not available and for that reason the out-of-core solver was used. The largest matrix that is stored in the DSIE approach is the MoM matrix for the first subsystem (1920 coefficients). It takes $m_{\text{DSIE}} = 59\,\text{MB}$. Therefore, the storage reduction in this example is $m = 61$ times.

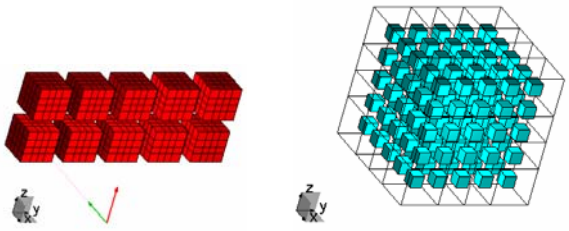

(a) (b)

Figure 8. (a) The exterior subsystem and (b) one of 10 congruent interior.

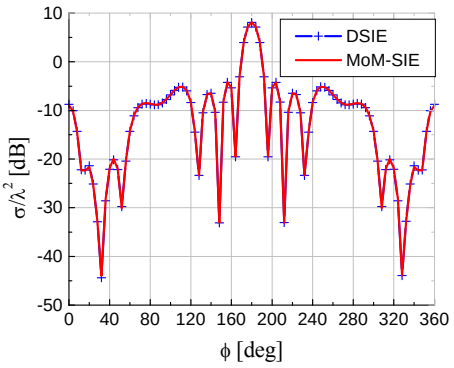

Figure 9. RCS calculated using DSIE vs. classical MoM/SIE: θ-cut.

VI. Conclusion

The diakoptic surface integral equation formulation is developed for efficient modeling of complex and large electromagnetic-field problems. The performance of the proposed technique has been demonstrated on various examples. Significant acceleration and storage reduction are achieved when compared to the classical solution of surface integral equations using the method of moments. Along with achieving the remarkably improved performance, the accuracy of the results is kept within acceptable limits.

The future work will include investigation of diakoptic boundaries with common walls, application of DSIE to optimization of complex EM structures and calculation of EM time-domain responses, and hybridization with other numerical techniques, such as finite elements and volume integral equation formulations.

Acknowledgements

The authors would like to thank Professor Dr. Branko Kolundžija for his help with WIPL-D code [6].

References

[1] R. F. Harrington, *Field Computation by Moment Methods*, New York: Macmillan, 1968. Reprinted by IEEE Press, New York, 1993.

[2] J. R. Mosig, "Integral-equation technique," in *Numerical Techniques for Microwave and Millimeter-Wave Passive Structures,* T. Itoh, Ed. New York: Wiley, 1989, ch. 3, pp. 133-213.

[3] T. K. Sarkar, A. R. Djordjević, and B. M. Kolundžija, "Method of moments applied to antennas", Chapter in *The Handbook of Antennas in Wireless Communications*, Ed. L. Godara, Boca Raton, Florida: CRC Press, 2001, pp. 8.1-8.41.

[4] B. M. Kolundžija and A. R. Djordjević, *Electromagnetic modeling of composite metallic and dielectric structures*, Boston: Artech House, 2002.

[5] A. R. Djordjević, M. B. Baždar, R. F. Harrington, and T. K. Sarkar, *LINPAR for Windows: Matrix Parameters for Multiconductor Transmission Lines* (software and user's manual), Artech House, Boston, 1996.

[6] B. M. Kolundžija, J. S. Ognjanović, T. K. Sarkar, M. Tasić, D. I. Olćan, B. Janić, and D. Šumić, *WIPL-D Pro. v5.1*, WIPL-D, 2004.

[7] B. Stupfel, "A Fast-Domain Decomposition Method for the Solution of Electromagnetic Scattering by Large Objects", *IEEE Transactions on Antennas and Propagation*, Vol. 44, No. 10, October 1996, pp. 1375-1385.

[8] B. Stupfel and M. Mognot, "A Domain Decomposition Method for the Vector Wave Equation", *IEEE Transactions on Antennas and Propagation*, Vol. 48, No. 5, May 2000, pp. 653-660.

[9] M. N. Vouvakis, Z. Cendes, and J.-F. Lee, "A FEM Domain Decomposition Method for Photonic and Electromagnetic Band Gap Structures", *IEEE Transactions on Antennas and Propagation*, Vol. 54, No. 2, February 2006, pp. 721-733.

[10] R. Coifman, V. Rokhlin, and S. Wandzura, "The Fast Multipole Method for the Wave Equation: A Pedestrian Prescription", *IEEE Antennas and Propagation Magazine*, Vol. 35, No. 3, June 1993, pp. 7-12.

[11] J. M. Song, C. C. Lu, W. C. Chew, and S. W. Let, "Fast Illinois Solver Code (FISC)", *IEEE Antennas and Propagation Magazine*, Vol. 40, No. 3, June 1998, pp. 27-34.

[12] S. Ooms and D. De Zutter, "A New Iterative Diakoptics-Based Multilevel Moments Method for Planar Circuits", *IEEE Transactions on Microwave Theory and Techniques*, Vol. 46, No. 3, March 1998, pp. 280-291.

[13] I. M. Stevanović and J. R. Mosig, "Using symmetries and equivalent moments in improving the efficiency of the subdomain multilevel approach," *IEEE Antennas and Wireless Propagation Letters.*, vol. 5, pp. 158–161, 2005.

[14] W. C. Chew, J.-M. Jin, and C.-C. Lu, E. Michielssen, J.M. Song, "Fast Solution Methods in Electromagnetics", *IEEE Transactions on Antennas and Propagation*, Vol. 45, No. 3, October 1997, pp. 533-543.

[15] K. C. Gupta, "Emerging Trends in Millimeter-Wave CAD", *IEEE Transactions on Microwave Theory and Techniques*, Vol. 46, No. 6, June 1998, pp. 747-755.

[16] W. C. Chew and C. C. Lu, "The Use of Huygens' Equivalence Principle for Solving the Volume Integral Equation of Scattering", *IEEE Transactions on Antennas and Propagation*, Vol. 41, No. 7, July 1993, pp. 897-904.

[17] C. C. Lu and W. C. Chew, "The Use of Huygens' Equivalence Principle for Solving 3-D Volume Integral Equation of Scattering", *IEEE Transactions on Antennas and Propagation*, Vol. 43, No. 5, May 1995, pp. 500-507.

[18] D. I. Olćan, I. M. Stevanovid, J. R. Mosig, and A. R. Djordjević "A diakoptic approach to analysis of large 2D problems", *2006 ACES Dig.*, Miami, FL, March 2006, pp. 527-531.

[19] D. I. Olćan, I. M. Stevanović, J. R. Mosig, and A. R. Djordjević, "Diakoptic surface integral equation gormulation applied to 3-D electrostatic problems", *Proc. of ACES 2007*, March 2007., Verona, Italy, pp. 492-498.

[20] D. I. Olćan, I. M. Stevanović, J. R. Mosig, and A. R. Djordjević, "Diakoptic approach to analysis of multiconductor transmission lines", *Microwave and Optical Technology Letters*, Vol. 50, No. 4, April 2008, pp. 931-936.

[21] D. I. Olćan, I. M. Stevanović, B. M. Kolundžija, J. R. Mosig, and A. R. Djordjević, "Diakoptic surface integral-equation formulation applied to large antenna arrays", *Antennas and Propagation Society International Symposium 2008*, San Diego, CA, July 4-12, 2008.

[22] D. I. Olćan, "Diakoptic analysis of electromagnetic systems," Ph.D. dissertation, Dept. Elect. Eng., Univ. Belgrade, Serbia, 2008.

[23] B. D. Popović, "Electromagnetic Field Theorems (A Review)" *Proceedings IEE*, Pt. A, 1981, pp. 47-63.

[24] R. F. Harrington, *Time-Harmonic Electromagnetic Fields*, New York: McGraw-Hill Book Company, 1961.

[25] L. Chua and L.-K. Chen, "Diakoptic and generalized hybrid analysis", *IEEE Transactions on Circuits and Systems*, Vol. 23, No. 12, December 1976, pp. 694-705.

[26] G. Kron, *Tensor Analysis of Networks*, John Wiley and Sons, New York, 1939.

[27] G. Goubau, N. N. Puri, and F. K. Schwering, "Diakoptic Theory for Multielement Antennas", *IEEE Transactions on Antennas and Propagation*, Vol. 30, No. 1, January 1982, pp. 15-26.

[28] A. R. Djordjević, T. K. Sarkar, "Transient analysis of electromagnetic systems with multiple lumped nonlinear loads", *IEEE Transactions on Antennas and Propagation.*, Vol.AP-33, No.5, May 1985, pp.533-539.

[29] F. K. Schwering, N. N. Puri, and C. M. Butler, "Modified Diakoptic Theory of Antennas", *IEEE Transactions on Antennas and Propagation*, Vol. 34, No. 11, November 1986, pp. 1273-1281.

[30] M. M. Nikolić, A. R. Djordjević, M. M. Nikolić, *ES3D: Electrostatic Field Solver for Multilayer Circuits*, Artech House, Norwood, MA, 2007.